Nonspecular meteor trail altitude distributions and durations observed by a 50 MHz high-power radar

G. Sugar,[1] M. M. Oppenheim,[1] E. Bass,[1] and J. L. Chau[2]

Received 20 May 2010; revised 4 October 2010; accepted 7 October 2010; published 30 December 2010.

[1] High-power large-aperture (HPLA) radars frequently observe nonspecular meteor trail echoes that result from plasma turbulence driven by the intense pressure gradients on the trail edges. This paper analyzes the altitude range, duration, and dependence on head echo strength of nonspecular trails using two large data sets from the 50 MHz HPLA radar at the Jicamarca Radio Observatory. Over 2100 trails were used to build altitude profiles that extend from 86 km to 120 km altitude, with 97% of events occurring between 90 km and 110 km. Longer-duration trails tend to form at lower altitudes than shorter-duration echoes. The peak of the altitude distribution of trails lasting at least 5 s can be up to 12 km lower than the peak of the distribution of trails shorter than 5 s. Further, the data show a clear power law relationship for the frequency of both head echo and nonspecular trail power. An improved knowledge of nonspecular trails will allow researchers to better understand meteor trail evolution and their use in monitoring lower thermospheric winds.

Citation: Sugar, G., M. M. Oppenheim, E. Bass, and J. L. Chau (2010), Nonspecular meteor trail altitude distributions and durations observed by a 50 MHz high-power radar, *J. Geophys. Res.*, *115*, A12334, doi:10.1029/2010JA015705.

1. Introduction and Background

[2] Millions of meteoroids barrage the Earth every second. As they move through the Earth's upper atmosphere, they collide with atmospheric molecules, become hot, and evaporate. Collisions between these liberated atoms and air molecules can cause the formation of a dense plasma column [*Ceplecha et al.*, 1998]. The steep pressure gradients on the edges of these columns supply free energy that generates waves and turbulence in the form of field aligned irregularities [*Oppenheim et al.*, 2003a, 2003b; *Dimant and Oppenheim*, 2006a, 2006b].

[3] Small radars detect specular meteor echoes when the pointing direction of the radar lies perpendicular to the meteor plasma column. Large radars, such as the one located at the Jicamarca Radio Observatory (JRO), detect meteor trails even when the specular condition is not met. Instead, they detect meteor induced plasma irregularities that cause Bragg scattering. The echoes are classified as either nonspecular [*Dyrud et al.*, 2002], range spread trail echoes [*Zhou et al.*, 2001], or spread meteor echoes [*Reddi et al.*, 2002]. For consistency, we will call them nonspecular trails for the remainder of the paper.

[4] Factors that determine where meteor trails form include atmospheric density and temperature, as well as the intrinsic properties of the meteoroid. Atmospheric properties, such as background electron density, vary substantially from day to night, so the experiments were conducted late at night until early morning in order to study the behaviors of trails in the two different environments. *Oppenheim et al.* [2008] showed that meteor trails are far more common and longer lasting at night than during the day. *Chapin and Kudeki* [1994, Figure 4] also show this trend. They provide a range-time intensity (RTI) plot showing data from 30 min before and after dawn on 14 August 1991 from the JRO that clearly shows the number of trails falling off dramatically after sunrise. It was argued that the greatly enhanced daytime ionosphere plasma density shorts out the meteor electric fields that play an integral role in driving instabilities [*Dimant and Oppenheim*, 2006a, 2006b]. The chemical composition of the meteoroid will determine the temperature at which the ablation process begins. Taking into account the meteoroid's size, velocity, and the background atmospheric properties, it may be possible to determine the chemical composition of the meteoroid from the altitude and duration of a trail [*Ceplecha and McCrosky* 1976].

[5] Using a small sample of ARPA Long-Range Tracking and Instrumentation Radar (ALTAIR) data, *Dyrud et al.* [2002] showed that meteor trails exist typically between 94 and 106 km altitude. The simple instability model developed by *Oppenheim et al.* [2003a, 2003b], combined with an ablation and ionization model, predicts this range fairly well [*Dyrud et al.*, 2005, 2007]. In this paper, we use much larger data sets from the JRO to show that while the altitude range of trails generally falls between 94 and 106 km, a smaller set of trails (19.3%) extend well above and below those altitudes from 86 km to 120 km. Recent developments by *Oppenheim et al.* [2009] have shown the importance of

[1]Center for Space Physics, Boston University, Boston, Massachusetts, USA.
[2]Radio Observatorio de Jicamarca, Insituto Geofísico del Perú, Lima, Peru.

0148-0227/10/2010JA015705

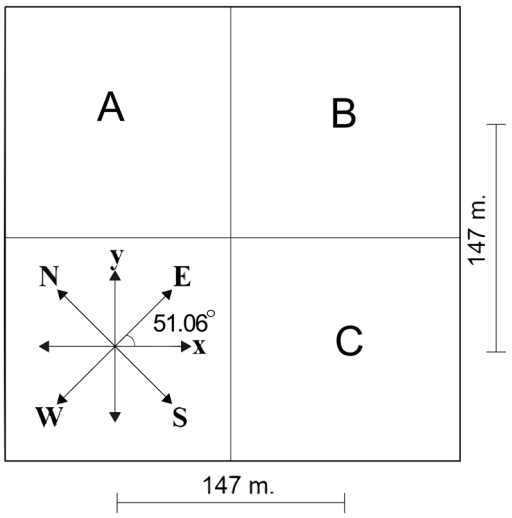

Figure 1. Antenna configuration for the Jicamarca Radio Observatory (JRO) radar. Notice the 51.06° rotation with respect to east-west. Figure modified from *Chau and Woodman* [2004].

trails in monitoring winds in the lower thermosphere. Better knowledge about where nonspecular trails form will help determine the extent that trails can be used to measure winds.

2. Data Collection and Analysis

[6] The data analyzed in this project were collected at the JRO in Peru from two experiments, one on 12 July 2005 and the other on 17 July 2007. The JRO operates one of the largest radars in the world, containing over 18,000 dipole antennas covering an area of almost 85,000 m^2 with a peak power of 2 MW [*Chau and Woodman*, 2004]. Both experiments applied a short, uncoded, 1μs pulse at 50 MHz broadcast from the entire antenna array, with a half-power beam width of ~1°. The uncoded pulse has the advantage that it returns a high-resolution echo without range-aliasing or range spreading at the cost of lower sensitivity than the coded pulse.

[7] For transmission, the JRO 50 MHz radar broadcasts a coherent, plane polarized, signal from the entire antenna array, while for reception, it was split into four quarters as shown in Figure 1. Echo amplitude and phase data were recorded independently from three of the four quarters (A, B, and C), allowing for interferometry. The position of a meteor is found from the phase difference of signals received in the different quarters.

2.1. Differences Between the Experiments

[8] Table 1 lists the differences between the two experimental setups. More specifically, the 2005 data set was initially sampled at 1 μs from 0341 to 0450 PET (UTC −5), and then changed to a 0.5 μs sampling rate from 0451 to 0850. This caused an increase in noise and about a 3 dB loss in sensitivity during the day measurements. In 2007, the antenna was positioned so that the aspect angle (the angle between the radar's line of sight and a vector perpendicular to the Earth's magnetic field) was 0°, causing the peak electrojet interference to run through the most sensitive part of the beam pattern. In the 2005 experiment, the antenna was positioned so the peak sensitivity of the beam lies 1.9° off B (the aspect angle). This configuration reduces electrojet signals by placing highly field aligned signals near a minimum of the beam pattern. Also, the 2007 experiment used new solid state amplifiers that improved the transmitter pulse.

[9] Only 29% of the 2005 data and 64% of the 2007 data were useful due to electrojet interference saturating the signal. Since the electrojet typically occurs in the middle of our observed range, between 90 and 110 km, including data with electrojet would bias our results to observe more trails at high and low altitudes. We used data from 0341 to 0450 and 0801 to 0821 on 12 July 2005 and between 0401 and 0612 and 0631 to 0715 on 17 July 2007. The 2007 nighttime data had weak but observable electrojet interference persisting between 95 km and 110 km, but we could still distinguish trails from electrojet through examination of the phase differences between channels. Trails are localized and have slow changing phase differences, while the electrojet is spread along the magnetic field lines and will not have a consistent phase difference. Nevertheless, weak head echoes could be missed in the electrojet since they are not as visible in RTI plots as trails. We will further discuss how this weak electrojet could have influenced our results in section 3.5.

2.2. Head and Trail Identification

[10] The data were manually examined to record each meteor head and trail. An example of a head and trail pair is given in Figure 2. Trails and heads were identified through manual inspection of the signal-to-noise ratio (SNR) (see Figure 2, top left). Noise was calculated by the method given in the work of *Hildebrand and Sekhon* [1974]. Typically, a clear gap with a reduced SNR exists between the head echo and the trail. We isolated each trail by putting a line through the head-trail gap and then marking the point at the end of the trail when the signal becomes indistinguishable from the background noise. When there was no distinguishable gap, we used the Doppler data to isolate the head from the trail. Head echoes typically have a rapidly changing Doppler due to deceleration, but the trail's Doppler remains relatively constant near 0 m/s (see Figure 2, top right).

[11] In order to remove secondary head echoes that often exist within longer trails, we used a Doppler filter on the trails, ignoring points having an absolute Doppler value greater than 150 m/s. The Doppler threshold eliminated most of the head echoes from within the trails, but some contamination was inevitable since the Doppler aliasing

Table 1. Experimental Setups

	2005	2007
Pulse width (μs)	1	1
Sampling rate (μs)	1 night, 0.5 day	1
Interpulse period (μs)	400	433
Range resolution (m)	150	150
Bottom altitude (km)	90.00	80.00
Top altitude (km)	119.25	129.75
Aspect angle (deg)	1.9	0
Time (PET)	0451–0850	0401–0832

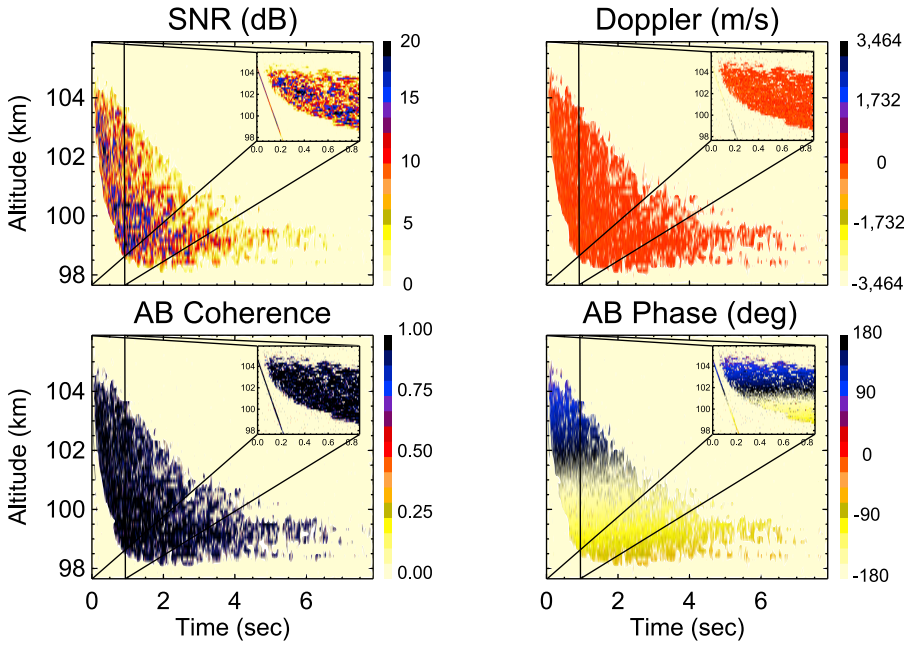

Figure 2. Images showing the head and subsequent nonspecular trail echo, showing (top) total signal-to-noise ratio (SNR) and Doppler of all three channels and (bottom) the AB cross channel coherence and phase difference. (inset) Expansion of the first 0.9 s to reveal the distinct head echo, the isolated diagonal line on the left. All data points where the SNR were below 0 dB were eliminated to hide the noise.

range is ±3464.2 m/s and head echoes frequently go through the entire Doppler range. If a head echo covered the entire Doppler range (3464.2 m/s through −3464.2 m/s), 95.7% of its signal would be filtered out. In the rare case that a secondary trail develops within a primary trail, we cut off the first trail where the second one began to prevent double counting. The number and frequency of observed trail and head echoes are given in Table 2. Trails lasting longer than 5 s were classified as "long duration", while those under 5 s were "short duration". A detailed explanation of the 5 s threshold is given in section 4.1.

[12] Approximately 19.5% of all the heads in our data sets produced trails. As one might expect, more energetic head echoes were more likely to produce trails. Figure 3 demonstrates this by showing the percentage of heads with a certain net power that produce trails. In contrast, *Zhou et al.* [2001] stated that for the MU radar using a 2 μs pulse at 46.5 MHz, nearly all head echoes were followed by a nonspecular trail. This discrepancy probably arises from the differences in radar configurations and analysis techniques. Unfortunately, the Zhou et al. paper does not describe their head or trail identification methods, nor did it give any statistical information about the observations. Without this information, it is impossible to determine the reason for the differences in the data. Through manual examination of a large amount of JRO data, we were able to identify many low power heads that generally did not produce trails. We suspect that the previous work missed these low power heads, causing the higher proportion of trail producing heads.

[13] In the process of analyzing the data, we observed atypical signals that immediately followed head echoes. One unusual signal was a streak of high SNR that immediately followed a head echo without a time gap. These were not included in our nonspecular counts but, since they constitute less than 1% of the population, this exclusion has no significant impact on our counts. These signals were also observed by *Malhotra and Mathews* [2009] and classified as Low-Altitude Trail Echoes (LATE) because they found them only at low altitudes. We observed two types of flares as well as two distinct populations centered at different altitudes, one at ~90 km and the other at ~112 km. Examples of these events are shown in Figure 4.

[14] One type of flare consists of an SNR streak restricted to an altitude range of less than 300 m (Figure 4a), while the other type has multiple streaks spread over a set of neighboring altitude ranges (Figure 4b). *Malhotra and Mathews* [2009] discussed only single streak flares which make up

Table 2. Number and Frequency of Trails and Heads Observed

	2005 Night	2005 Day	2007 Night	2007 Day
Observed time (min)	69	20	129	44
Heads	4926	1225	3483	1528
Heads/min	71.4	61.3	27.0	34.7
All trails	1143	45	888	99
All trails/min	16.6	2.3	6.9	2.3
Percent of heads with trails	23.2%	3.7%	25.5%	6.5%
Short trails (<5 s)	1032	43	811	91
Short trails/min	15.0	2.2	6.3	2.1
Percent of heads with short trails	21.0%	3.5%	23.3%	6.0%
Long trails (≥ 5 s)	111	2	77	8
Long trails/min	1.6	0.1	0.6	0.2
Percent of heads with long trails	2.3%	0.2%	2.2%	0.5%

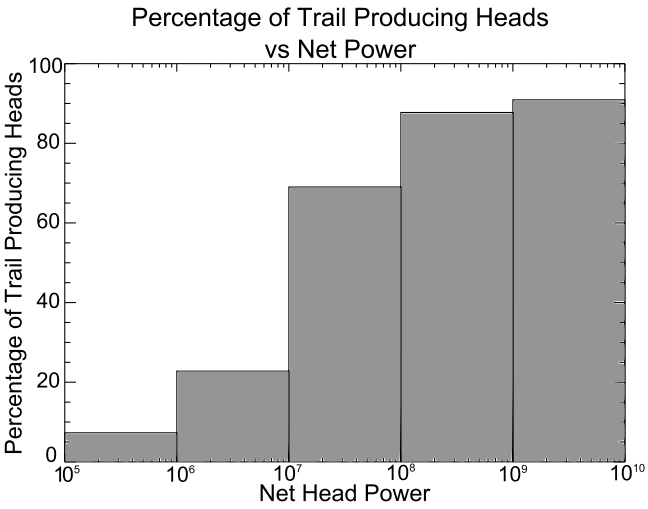

Figure 3. Percentage of trail-producing heads versus total head power of the associated head echo in JRO Watts. We use JRO Watts as an arbitrary measure of power which remained consistent for all experiments because an accurate calibration was difficult and not essential. Notice the sharp drop in percentage below 10^7 JRO Watts.

the majority of the population centered at 90 km, although some were observed above 110 km. The multiple streak flares usually occurred at higher altitudes, although a few were observed at the lower altitude range. Because the isolated streak signals do not happen exclusively at low altitudes, LATE is not an appropriate name. We will call them, as well as the multiple streak events, "head echo flares", due to the appearance of a signal coming off the head immediately. Table 3 shows number and frequency of flare observations for each data set.

[15] There were significantly more head echo flares in 2007 than in 2005. This is probably due to the different

Table 3. Number and Frequency of Head Echo Flare Observations

	2005 Night	2005 Day	2007 Night	2007 Day
Flares observed	10	6	13	65
Percent of heads with flares	0.20%	0.49%	0.37%	4.25%

ranges of observed altitudes in the experiments. The minimum altitude in 2005 was 90.00 km, while in 2007 it was 80.00 km. Therefore, we would miss approximately half of the flares in the population centered around 90 km in 2005.

[16] We can speculate the reasons for the lack of a time gap between the signal and the head. The plasma may become turbulent much faster than usual because a rapid nonuniform release of material. *Malhotra and Mathews* [2009] argue that this results from fracturing of the meteoroid. Assuming this causes a rapid increase or decrease of plasma created over a small distance (not much more than a few times the mean free path), this could substantially enhance the irregularity growth rate. However, one would expect that high-resolution, short-pulse experiments like these and the ALTAIR measurements would then observe a second head echo moving away from the first since these radars resolve 150 m and 30 m, respectively, and the head echoes would decelerate at different rates. The authors have never seen such observations. Differential ablation could cause flares, but that process may be too gradual to explain the sharpness of the isolated streak observations. We propose a third mechanism. Some meteoroids contain pockets of material with lower sublimation temperatures and when the covering layer disappears exposing this material to space, it quickly sublimates and ionizes, creating a burst of high-density plasma and rapid generation of irregularities. Whatever the reason, flares clearly differ from nonspecular trails and are very rare. Only 0.84% of heads have flare echoes, as opposed to the 19.49% that produce nonspecular trails. Our set of flares also exhibit the opposite day/night dependence, with a higher frequency during day than at night. We are

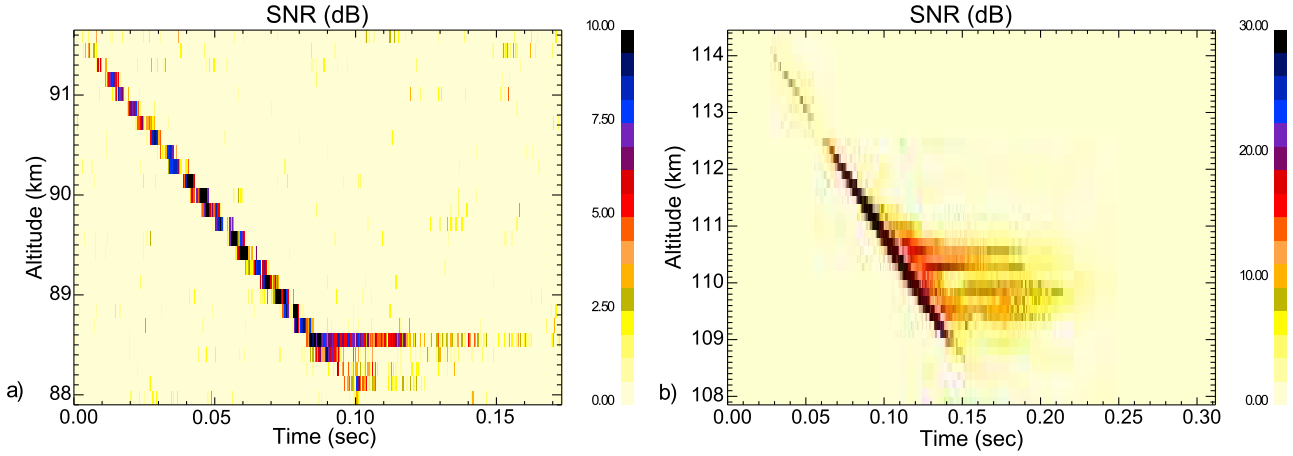

Figure 4. Examples of flares, showing (a) a typical single streak flare and (b) a typical multiple streak flare. There is no gap in signal between the streaks and the head echo. The rarity of these signals suggests that something unusual is happening. The immediacy of the signal following the head echo implies that something initiates the plasma irregularities and that they do not grow from a smooth column, as we believe is the case for typical nonspecular trails.

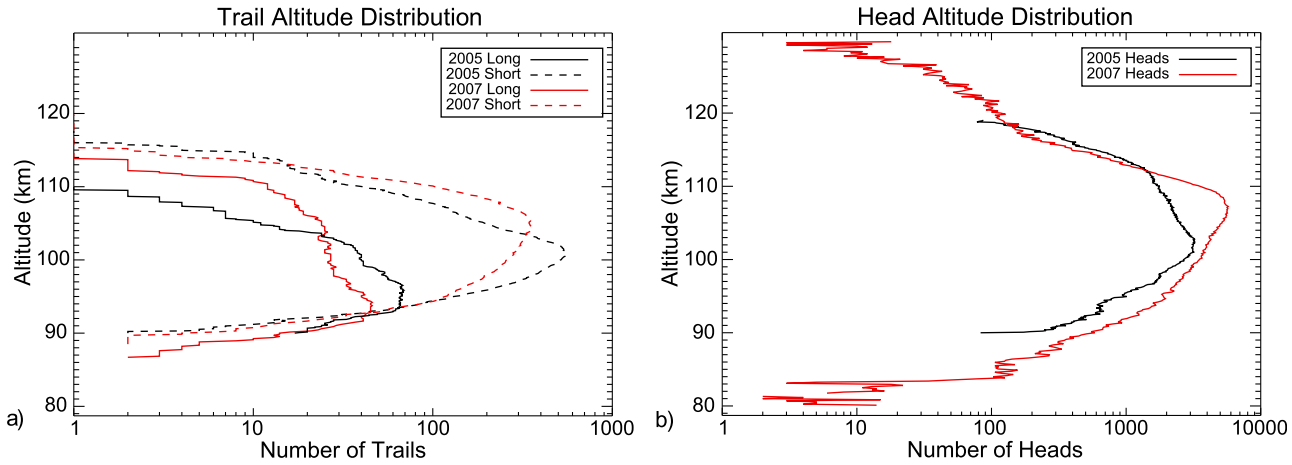

Figure 5. Number of observed (a) nonspecular trails and (b) heads at each altitude. We do not display day and night data sets separately because the limited sample size of the daytime trails causes too much noise in the distributions. Statistics for day and night trail distributions are given in Tables 4 and 5. Range and altitude are equivalent to within 0.2% because of the small off-vertical angles and the narrow beam pattern.

currently analyzing the flares to explore day/night variations, altitude distributions, and possible sources.

2.3. Possible Bias in Data Collection

[17] The process of manually examining the data to extract heads and trails took hundreds of hours. Some sections of the data may have been examined more closely than others, causing more echoes to be observed during certain times. In order to minimize any bias, we used an automated filter that ignored any data points with a cross-channel coherence less than 0.97. In order for a trail to be counted, it had to have at least one altitude where there were five valid data points within 0.12 s of each other. This filter threw away 8.2% of 2007 trails and 36.4% of 2005 trails, all of them short duration.

[18] The greater percentage of trails that failed to meet the thresholds in 2005 could be cause for concern. However, the 2005 nighttime set had a 0.5 μs sampling rate, as opposed to 1 μs in 2007. The faster sampling rate increases the noise and decreases sensitivity by ~3 dB. 96% of the 2005 trails were observed with the 0.5 μs sampling rate. The increased noise would lower the cross channel coherence and therefore decrease the number of trails that meet the filter thresholds. We explain the small but understandable differences between the results of the filtered and unfiltered data in section 3.7.

3. Results

[19] The large sample size of over 2100 trails enabled us to generate altitude distributions using the number of trails observed and the net power of the trails. Analysis of these distributions showed a strong correlation between head and trail power, a preference for long-duration meteors to form at low altitudes, and a minimal difference between the filtered and unfiltered data results.

3.1. Altitude Distributions

[20] We characterize the trail altitude distribution by counting the number of trails (Figure 5) and summing the trail power at each altitude (Figure 6). We use the net power, rather than the mean or maximum power, because it characterizes the trail strength with the least influence of arbitrary selection criteria or contamination by nontrail signals. The mean power depends strongly on the manually determined duration of the trail, while the maximum power can be modified by strong transient surges in their signal strength or by a head echo embedded in a trail. Table 4 gives the peak altitude for the trail distributions in Figure 5a, and Table 5 gives the means and standard deviations.

3.2. Head and Trail Power Relationship

[21] The distributions in Figures 5 and 6 show that while head echoes are observed over a larger range than trails (heads were observed from 80 km to 129 km and trails just from 86 to 120 km), high-power heads and high-power trails are observed at similar altitudes. One would expect that a strong head echo will create a strong and long-lasting trail. A strong head echo indicates the deposition of an above average amount of energy and plasma, which should drive stronger and more persistent waves. Figure 7 displays the head power, trail power, and mean head altitude for each trail. Notice the strong correlation between head and trail power, as well as the influence of altitude.

[22] The data show a relationship between the trail power summed over all trail data points p_t, the head power summed along the line of head echo data points p_h, and the mean altitude of the trail z (in kilometers), such that

$$p_t = A\left(\frac{p_h}{p_{ho}}\right)^B\left(\frac{z}{z_o}\right)^C$$

where p_{ho} and z_o are normalization factors of 1 JRO Watts and 1 km, respectively. Regression analysis gives the coefficients: $A = 5.082 \times 10^{35} \pm 1.052 \times 10^{35}$ JRO Watts, $B = 0.789 \pm 0.015$, $C = -16.188 \pm 0.625$. The correlation coefficients for B and C are 0.707 and −0.382, respectively.

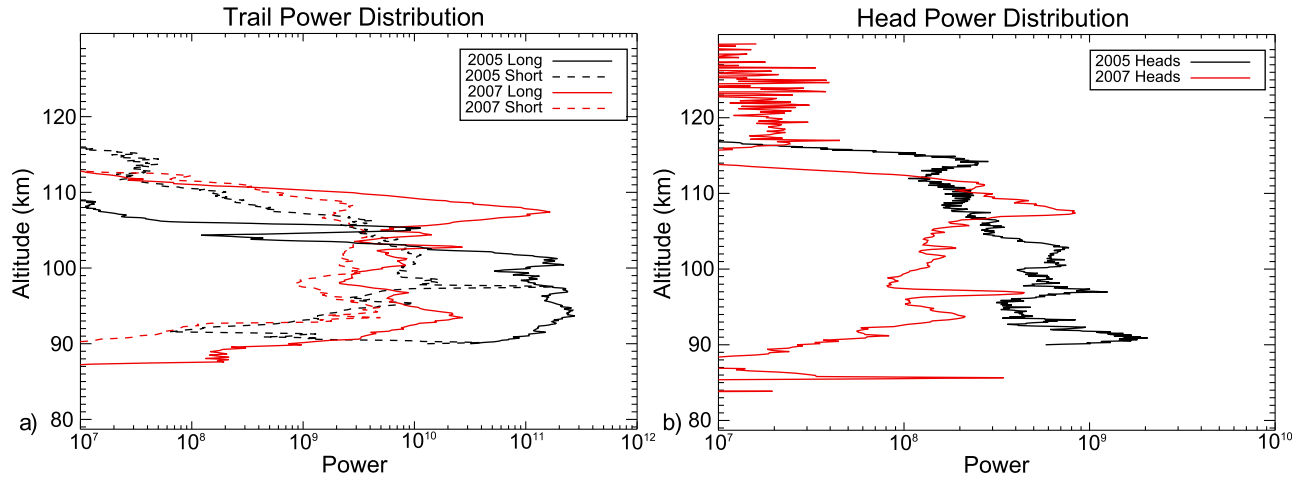

Figure 6. Net power at each altitude for (a) nonspecular trails and (b) head echoes. The trails were separated into two groups, namely trails less than 5 s (short trails) and trails greater than 5 s (long trails). The trail distributions were generated by summing the power of each trail at each altitude individually after the Doppler filter described in section 2.2. No filter was used for the head distributions. The day and night sets are combined for each year. The noise in the peak power results from a few very strong trails or heads. The short trail power shows considerable noise because of the dominance of trails between 4 and 5 s duration.

[23] In general, a strong head at high altitude is likely to form a strong trail, while a weak head at low altitude generally will not. The large magnitude of C occurs because a few percent change in altitude correlates with orders of magnitude power changes. The low correlation value for C results from the high scatter in power for a given power and altitude. Analysis of trails with head powers limited to between 3×10^6 and 4×10^6 gave a correlation value of -0.588 for C, showing a stronger relationship between altitude and trail power. The larger correlation coefficient for head power could also be influenced by the beam pattern since 10–15% of head echoes are found in side lobes outside of the main beam [*Chau et al.*, 2009]. These side lobes are ~17 dB less sensitive, so what would normally be a strong head-trail pair would yield much less power. Since the JRO 50 MHz radar has interferometric capabilities, an analysis that accounts for meteor position should be possible.

3.3. Long and Short Trail Distribution Differences

[24] There is a noticeable difference in the altitude distributions between long-duration and short-duration trails. In 2005, the long-duration peak was 5 km lower than the short-duration peak. In 2007, the long-duration peak was 12 km lower. Doing a Welch's t test on the short and long-duration 2005 trails gave a t value of 15.00, meaning there is a significant difference in the means with over 99.99% certainty. The same test on the 2007 set gave a t value of 9.43, also yielding over 99.99% certainty. The t tests show that there is overwhelming statistical evidence that long-duration trails form at lower altitudes than short trails. The count distributions in Figure 5a also show a clear preference for long-duration trails to form at low altitudes, with the majority of 5+ s trails occurring below 97 km.

[25] The power distributions in Figure 6a do not show the low altitude preference for long-duration trails as clearly and instead show the complexity of trail formation and evolution. The plots are dominated by the longest of trails because they have more data points than shorter trails and generally higher SNRs. Even the "short trail" distributions are dominated by the longest trails that last between 4 and 5 s. There are 1075 short trails in 2005, and only 37 last between 4 and 5 s. These 37 trails cause the multiple peaks in the 2005 short distribution. While the count distributions in Figure 5a clearly show the preference for long-duration trails to form at low altitudes, a few long-duration trails that at high altitudes dramatically impact the total trail power. Long trails contain orders of magnitude more power than short trails, which is why their distributions have more power at almost all altitudes than the short ones, despite their being just ~9% of all observed trails.

Table 4. Peaks of the Number of Trails Observed Altitude Distributions

Type of Trail	2005 Night	2005 Day	2007 Night	2007 Day
Short trails (<5 s)	101 km	98 km	105 km	102 km
Long trails (≥ 5 s)	96 km	94 km	93 km	101 km
All trails	101 km	98 km	105 km	102 km

Table 5. Mean and Standard Deviation for the Number of Trails Observed Altitude Distributions

	Short Trails (<5 s)	Long Trails (≥ 5 s)	All Trails
2005 night mean	101.1 km	97.2 km	100.6 km
2005 night SD	3.8 km	4.0 km	4.0 km
2005 day mean	97.8 km	95.6 km	97.6 km
2005 day SD	4.5 km	3.3 km	4.5 km
2007 night mean	102.7 km	98.3 km	102.2 km
2007 night SD	4.6 km	6.1 km	5.0 km
2007 day mean	101.9 km	100.4 km	101.7 km
2007 day SD	3.7 km	4.9 km	3.9 km

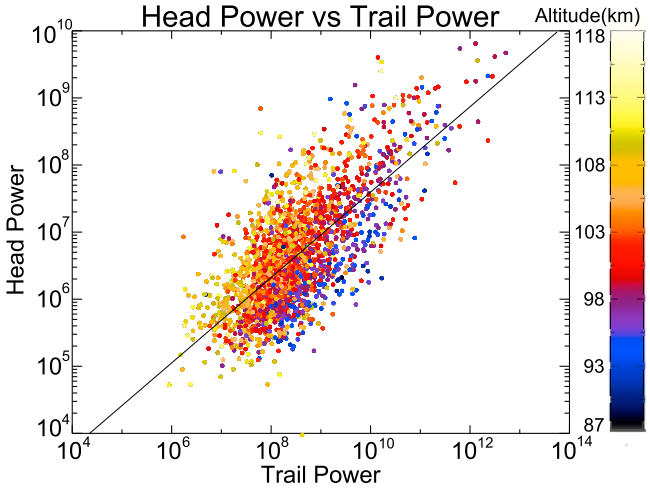

Figure 7. Head power, trail power, and mean altitude for each head/trail pair with a least squares fit. Each point corresponds to a single trail. The power was calculated by summing the power of all data points for a given trail at each altitude. Notice the pattern of decreasing altitude as the head power is held constant and trail power increases.

3.4. Power Law Relationship Between Radar Power and Meteor Frequency

[26] The dominance of a few strong and long trails on the power distributions will persist regardless of the size of a data set. Despite the infrequency of long-duration trails, such trails will contain more power than many small ones combined and will impact power analyses such as in section 3.1.

[27] We have found a simple power law relationship between the number of trails and the trail total power. As seen in Figure 8, this relationship exists for all data sets, with similar slopes and applies over three decades of power, from 10^8–10^{11} JRO Watts. This relationship changes at low power where radar sensitivity diminishes, while at high power, the sample size becomes too small for statistical relevance.

[28] The power law relationship suffers from the problem that no matter how much data is used, a few heads or trails with dramatically more power than the majority will dominate the power-altitude distributions. Figure 9 shows both the head power distribution and the cumulative distribution for direct comparison with Figure 8.

[29] Since both power law distributions are remarkably constant over 3 orders of magnitude, we fit a line to heads with powers between 10^6 and 10^9 JRO Watts. Assuming the equation $N = Ap_h^B$ where N is the number of observed heads and p_h is the head power, we found values of $A = 1.20 \times 10^8 \pm 2.3 \times 10^7$ and $B\ e = -0.72 \pm 0.01$. We ignored heads with power below 10^6 JRO Watts because they have a weak signal and many might have been missed during the collection process. We ignored heads with power above 10^9 JRO Watts because of the small sample size.

3.5. Trail to Head Ratio

[30] In order to remove bias due to the variability of meteor flux, we look at the trail to head ratio. Head echoes are the sole provider of opportunities for trail formation, and any change in their frequency will cause a similar change in the number of trails observed. There was significant variability in the head echo frequency between the two experiments. There were 69.1 heads/min in 2005 but just 29.0 heads/min in 2007. There is evidence that there can be significant annual variability in the sporadic meteor population. *Campbell-Brown and Jones* [2006] show up to a 50% annual variability in sporadic meteor observations. The maximum variability occurs in July, which happens to be the month of our experiments. However, annual variability cannot account for the 58% decrease in the number of heads echoes per minute from 2005 to 2007. The additional difference could be due to the weak electrojet in the 2007 data that increased noise and caused fewer heads to be observed. A weak head without a trail might have gone unnoticed, while a similar head with a trail would be easier to see and would be analyzed. This would lower the number of observed heads while increasing the percentage of heads that produce short-duration trails, both of which are observed in the data. Figure 10 displays the head to trail ratio for each altitude.

[31] Figure 10 shows both the tendency of long-duration trails to form at low altitudes and the absence of trails above 120 km and below 86 km. This lack of trails exists despite the presence of 197 heads above 120 km in both experiments and 20 heads below 86 km in the 2007 experiment (the 2005 run did not observe below 90 km). Using the percentages given in Table 2, we would expect 38 trails above 120 km and 4 below 86 km. This implies that trail formation is suppressed at high and low altitudes.

[32] The trail to head ratio was 0.232 in the 2005 night and 0.255 in the 2007 night, and the daytime ratios were 0.037 in 2005 and 0.065 in 2007. The daytime ratios are lower because of the increased rate of trail formation during the night. Assuming atmospheric properties were similar for both July experiments, the slightly higher overall ratios in 2007 are explained by the experimental setups. In the 2005 night, the sampling rate was 0.5 μs, half the rate in 2007, causing an increase in the noise and approximately a 3 dB drop in sensitivity. Also, in 2007 the radar was phased perpendicular to the Earth's magnetic field, but it had an

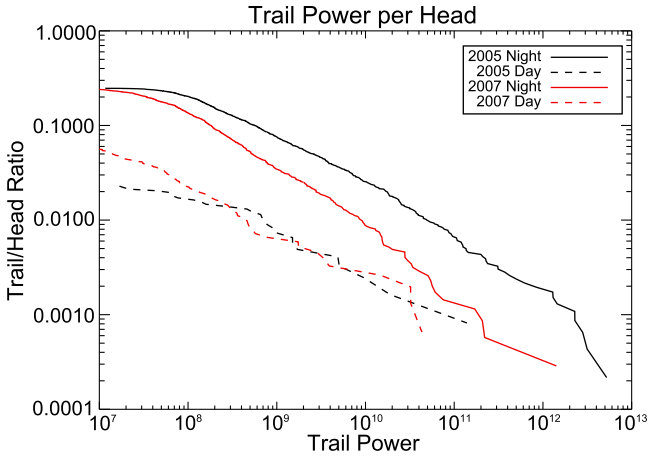

Figure 8. Fraction of head echoes having a trail of at least a given power for the four data sets.

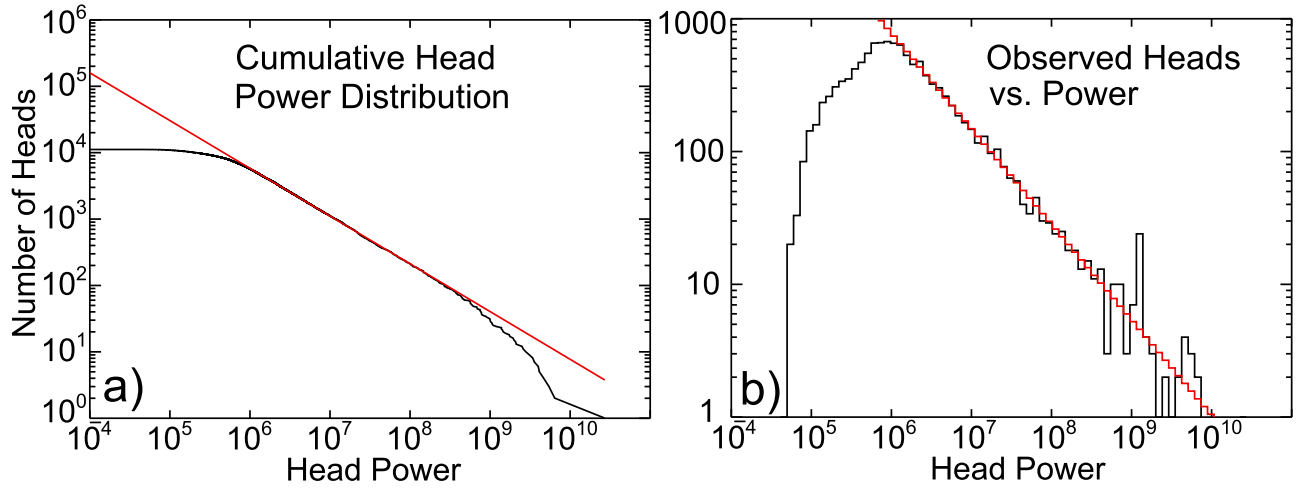

Figure 9. (a) Cumulative head power distribution and (b) a head power histogram. For the cumulative distribution, the number of heads represents the number of heads of at least a given power. For the histogram, the vertical axis shows the number of heads within the specified power range. The red line in Figure 9a was calculated through regression analysis on the cumulative data. In Figure 9b the red line shows data generated from the cumulative fit. Notice the strong agreement over three orders of magnitude between 10^6 and 10^9 JRO Watts.

aspect angle of 1.9° in 2005. Because theory predicts trails to be somewhat field aligned, weak trails observed in 2007 might have fallen below the detection threshold in 2005, causing the head to trail ratio to be lower in 2007. However, the small difference between the 2005 and 2007 ratios indicates that these have little effect. Differences in the head to trail ratios between day and night most likely result from the increased background electron density affecting the plasma trail diffusion [*Oppenheim et al.* 2008].

3.6. Day and Night Altitude Distributions

[33] The day and night distributions show distinct differences in their peak altitudes (see Tables 4 and 5); however, the small daytime sample sizes and the change in the 2005 data sampling rate prevents us from drawing definitive conclusions. There were only 144 trails in both 2005 and 2007 daytime sets combined, compared to 2031 total nighttime trails. A Welch's t test gave a 99.94% likelihood that the 2005 day/night altitude difference of 3 km was not due to the inherent randomness of the individual events. The same test on the 2007 data gave only a 49% certainty that the 1 km altitude difference is statistically significant.

[34] The 2005 altitude difference may have resulted from the faster sampling rate during the 2005 night, causing weak trails to be missed. Since weak trails preferentially form at high altitudes, missing these would cause the mean nighttime altitude to drop. Therefore only the 2007 experiment could be used for a day-night comparison, but the sparse daytime data reduces the certainty substantially.

3.7. Filtered and Unfiltered Data Results

[35] There are small but understandable differences between the filtered and unfiltered data. The long-duration distributions were not affected at all, and the short-duration distributions changed minimally. The peaks of the count distributions do not change significantly for the 2007 sets or the 2005 night set, but the filtered 2005 day short trail set peak is ~3 km lower than the 2005 day unfiltered distribution. The mean values of the distributions all decreased: 2.9 km for the 2005 night, 2.7 for the 2005 day, 1.8 for the 2007 night, and 0.3 for the 2007 day. We would expect the filter to lower the mean altitudes but not the peak because only the shortest of trails were filtered out. These trails are inherently the weakest and provide the lowest cross channel

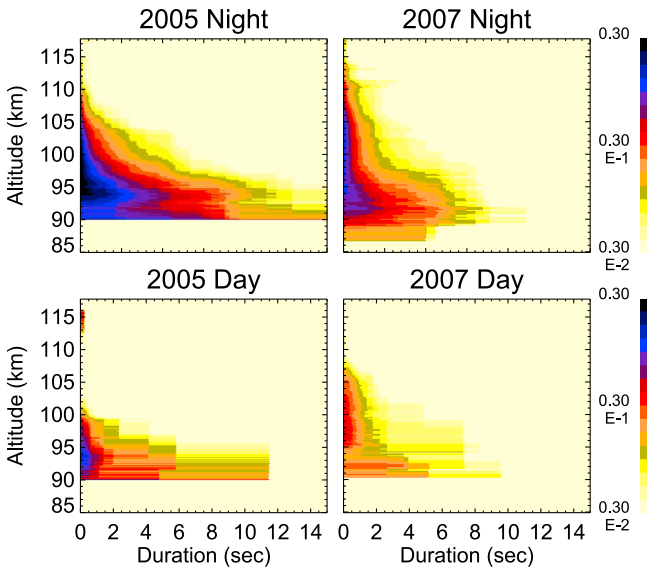

Figure 10. Fraction of heads with associated trails that persist for a given duration at a particular altitude. The images were made by analyzing each altitude separately and dividing the number of trails that last at least a certain duration by the number of head echoes observed at that altitude.

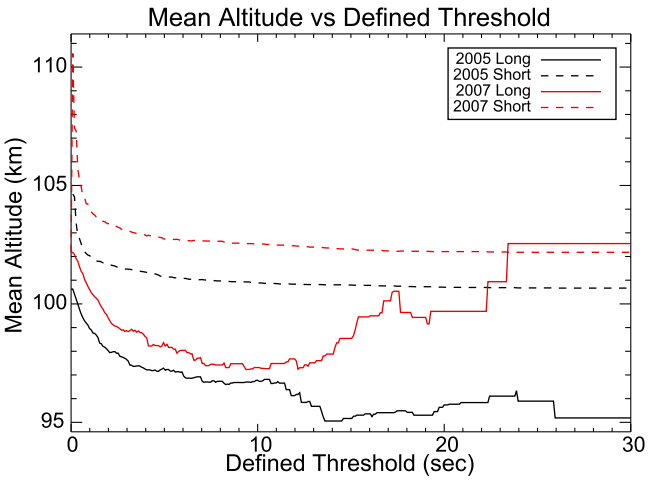

Figure 11. Change in the mean altitudes for long and short duration trails of the 2005 and 2007 night data sets as the threshold for classifying long/short trails changes. There are seven trails that last longer than 30 s, but we cut the duration axis short for scaling purposes.

coherence. We expect these trails to be at high altitudes, so it is understandable that when filtered out, the mean altitudes would be lower. The peaks would be unaffected because almost all of the filtered trails would be at altitudes above the peak. Because there were no unexpected differences between the filtered and unfiltered results, we conclude that there was minimal bias introduced in the manual extraction of head echoes and trails from the data.

4. Discussion

[36] These large nonspecular trail data sets enable us to perform not just statistical analysis of the altitude distributions but also analyze the magnetic field alignment dependence of the trails due to the different pointing direction of each experiment. In this section we discuss the reasons for choosing the 5 s threshold for classifying long-duration trails and the field dependence of trails, as well as explanations for the results.

4.1. Long Trail Duration Threshold

[37] The duration threshold for classifying long versus short trails is rather arbitrary. Previous literature has the cutoff varying from 15 s [*Chapin and Kudeki*, 1994; *Malhotra et al.*, 2007] to over a minute [*Dyrud et al.*, 2007]. We analyzed long and short trails separately because of their different altitude distributions. We used various thresholds to find any drastic changes in the results. Figure 11 shows the change in the mean altitudes for short and long trails as the duration threshold for classifying long trails changes. We only show the night sets because the small sample size of the day sets do not show a clear trend, especially when compared to the data obtained at night. Figure 11 shows that the threshold should be greater than 2 s, since at that point the short-duration mean altitudes begin to plateau.

[38] Figure 11 shows some interesting trends. First, the sharp drop in mean altitude in the first two seconds implies that trails less than 2 s in duration preferentially form at higher altitudes. Since the data sets contain large numbers of trails between 0.1 and 2 s, this is a well resolved feature. Therefore the evolution of short and long trails may be substantially different. Second, notice how both the long and short mean altitudes decrease as the duration threshold increases from 2 to 12 s. As the duration threshold increases the shorter long trails move into the short-duration group, the long trail group shrinks. This trend suggests that the longer the trail, the more likely it is to be found at a low altitude. This general rule seems to be violated after 12 s for the 2007 set. However, just 31 trails last longer than 12 s in the 2007 night, and a sample size this small cannot provide an accurate mean altitude.

[39] Comparing the number of trails that last for a minimum amount of time to the number of head echoes for each data set shows a distinct pattern as seen in Figure 12. As in Figure 11, a distinct change occurs at ~2 s. Before this time, the distribution function has a far steeper slope than for longer trails, though both show a simple exponential decay in the number of trails observed per time. We performed a fit on the combined nighttime data to find R, the trail/head ratio of trails lasting a minimum time t where we assume $R = Ae^{-t/t_o}$. Because of the drastic change in slope at 2 s, we found separate fits for the data between 0 and 2 s and 3+ seconds. Before 2 s, the regression finds $A = 0.248 \pm 0.001$ and $t_o = 1.162 \pm 0.004$ s, while after 3 s, it gives $A = 0.058 \pm 0.001$ and $t_o = 6.297 \pm 0.055$ s. The over 5 times slower decay rate for long-duration trails may indicate a change in the physics of trail diffusion and turbulence, perhaps the result of chemical evolution or dust formation in the plasma [*Kelley*, 2004]. The relatively constant slope after 2 s indicates that beyond this time, the point dividing long and short trails is somewhat arbitrary. We choose 5 s because it substantially exceeds 2 s but is short enough that we still have many long trails.

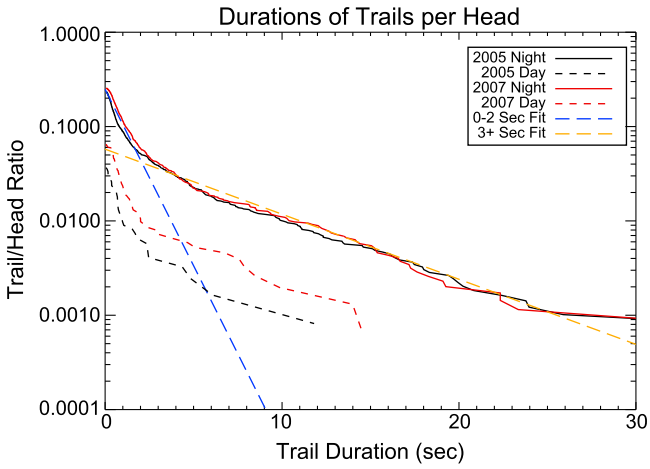

Figure 12. Fraction of head echoes having a trail persisting for a given time for the four data sets. Fitted lines are shown for 0–2 s and 3+ s for the ratio of the night sets combined. The "trail/head ratio" is the cumulative number of trails that last for at least the time indicated divided by the number of heads observed for the data set. Note that there are four trails that last longer than 30 s in the 2005 night and three in the 2007 night but none during the daytime observations.

4.2. Magnetic Field Dependence of Trails

[40] The major difference between the two experiments was the pointing direction of the radar, which allows for analysis of the field aligned dependence of trails. In 2005, the radar was phased to minimize its sensitivity to field-aligned plasma irregularities by lining up a null in its beam pattern with the direction perpendicular to the geomagnetic field. To do this, the center of the beam looked at waves with a 1.9° aspect angle. Using ALTAIR's 160 MHz radar, *Close et al.* [2008] found that radar sensitivity to nonspecular trails falls off approximately 3 dB ± 2 dB per degree as the radar points progressively away from perpendicular to **B**. This means that moving the center of the beam from 1.9° off perpendicular to **B**, as done in 2005, to 0°, as in 2007, will have probably less than a 3 dB reduction in sensitivity, a change that will mostly affect weak and short trails.

[41] Our analysis of the dependence of nonspecular trail sensitivity on the aspect angle is limited by the rather small 1.9° difference, as well as the different pulse durations between the two experiments. The 2005 night set sampled at a rate of 0.5 μs instead of 1.0 μs, causing a 3 dB reduction in sensitivity. Ignoring the daytime data because of small sample sizes, there is only a 0.1% difference between the percentage of heads that produced long-duration trails in 2005 and 2007 nighttime and a 2.3% difference between the short-duration percentages. These variations are not statistically significant and are too small to determine if there was any sensitivity loss due to the small change in aspect angle. Another data set with the radar observing at a larger aspect angle with respect to **B** and constant pulse durations could measure the effect of radar pointing direction on sensitivity to nonspecular trails.

4.3. Explanation of Low-Altitude Preference for Long-Duration Trails

[42] We stated in section 3 that long-duration trails tend to be found at lower altitudes than short ones. This result can be explained by the higher background density at lower altitudes. The high background density will cause more collisions with the plasma, slowing the diffusion and causing the plasma to remain confined to a smaller volume. This will result in a spectrally broad reflected signal that is observable to both the 2005 and 2007 radar configurations. While the high density slows diffusion and causes the trail to last longer, it also causes the received signal to be less restricted to magnetic field alignment. *Dyrud et al.* [2007] provides a more detailed explanation on these processes.

[43] In discussing the field alignment of long-duration trails, one must consider both that trails evolve over time as discussed by *Dimant and Oppenheim* [2006a, 2006b] and that atmospheric winds will transport them substantial distances during observations [*Oppenheim et al.*, 2009]. For example, a 150 m/s meridional wind can transport a 20 s trail 3 km, clear across the JRO beam pattern. If radar sensitivity to trail echoes spans a few degrees of aspect width as suggested by the *Close et al.* [2008] result, the echo might initially come from a sidelobe but then be transported to an off-center region of the beam pattern which maximizes the sensitivity and irregularity strength. Particularly in the case of radar with antenna arrays such as JRO, the sensitivity pattern will be a convolution of the complex beam pattern with the irregularity position and aspect width. One would expect to occasionally see long trails without head echoes because the plasma column initially falls in a null and then, as the wind moves the plasma into a sensitive part of the beam it appears. Likewise the plasma irregularities turbulence can extend along **B**, well beyond the plasma column, and be observed. Indeed, we do occasionally observe trails without heads and rather oddly shaped trails that may result from these effects.

4.4. Explanation of Altitude Distribution Differences Between Experiments

[44] The 2.9 km nighttime and 7.1 km daytime increase in mean trail altitudes observed between 2005 and 2007 could result from several causes. The primary cause may be that the 2007 data collection technique was between 4 and 8 dB more sensitive, as discussed in section 4.2, and one would expect a higher fraction of short trails from the more sensitive observations. In this case, the mean altitude should move up since the average short trail occurs at higher altitudes.

[45] A higher mean trail altitude in 2007 would occur if trails become progressively more field aligned with increasing altitude. This seems plausible since, as the collisional mean free path becomes longer, trails spread out faster and the irregularities become spectrally narrower faster. The 2007 data set was more sensitive to field-aligned irregularities and would observe more of these events than the 2005 data set.

[46] A third possible cause of the altitude difference could result from changes in the neutral atmosphere. We know that the winds can reach 150 m/s and change dramatically over a few kilometers altitude [*Larsen* 2002, *Oppenheim et al.*, 2009]. This peak velocity represents more than half the speed of sound and can move up or down by a number of kilometers over the course of the day. These winds and shears will certainly impact the evolution of the meteor plasma turbulence responsible for nonspecular echoes.

[47] Neutral densities can also influence the mean altitudes. If, during one experiment, the density were substantially higher than during the other, then meteoroids would ablate at a higher altitude and the altitude distributions would be shifted up. Using the MSIS-E-90 atmosphere model, we found up to a 20% day to day variability in the neutral density at 100 km above the JRO in the month of July, which would cause a ~2 km shift in both head and trail altitudes [*Hedin*, 1991]. While the day to day variability can be drastic, the MSIS model predicts similar densities to be 0.7 km higher in 2007 than in 2005. Since MSIS gives typical densities, we argue that the 20% day to day variability probably better reflects the true variability.

[48] Figure 5b shows that the mean head echo altitude for 2007 also occurs 5–8 km higher than in 2005. This increase of almost an entire scale height exceeds the expected level of variation and it must be combined with other effects to explain the altitude differences between the experiments. Variability in the meteoroid population may also affect the mean altitudes. If the meteors during the 2005 measurements were appreciably heavier or denser on average than the 2007 ones, that would cause them to penetrate deeper into the atmosphere and force the peak altitudes down. It would also cause them to have longer lived trails. Although

these measurements were taken at approximately the same time of year, we do not yet know how much mass variability in the sporadic population exists on a year-to-year basis.

5. Summary

[49] We analyzed over 2100 nonspecular trails to generate altitude distributions that agree with models and previous experiments. While the peaks of the distributions may shift a few kilometers depending on the time of day, atmospheric properties, and pointing direction of the radar, we are confident in our claim that the ideal range to observe trails is 86 km to 120 km. This range encompasses all trails observed in the four data sets. If this analysis is repeated using additional data sets, it may be possible to infer atmospheric properties based on the changes of the altitude distribution peak. This could be done by comparing altitude distributions from experiments conducted when atmospheric properties are well known. We also examined the durations of the trails and concluded that beyond 2 s there is no distinct threshold to classify long-duration trails, but there is a difference in behavior between longer and shorter trails. The data show a power law relationship between trail power, head power, and altitude, with a clear preference for high-power trails to form at lower altitudes and have high-power head echoes.

[50] Our results come from data obtained using a 50 MHz radar running with a short, uncoded, 1 μs pulse. Radars using different frequencies may observe slightly different altitude distributions because they are sensitive to different wavelengths in the turbulent plasma. In particular, as one uses higher frequencies, the peak and average altitude will move down because short wavelength irregularities become less abundant at higher altitudes where the mean free path becomes longer. Conversely, lower frequencies will no doubt measure trails at higher altitudes. However, the overall trends we found, such as the low-altitude preference for long-duration trails and the strong correlation between head power and trail power, should be evident in nonspecular trail observations using different radars. More experiments should be conducted at a different time of year to examine the seasonal variability of the altitude distribution and determine to what extent atmospheric properties affect the distributions.

[51] **Acknowledgments.** Work was supported by National Science Foundation grants ATM-9986976, ATM-0332354, ATM-0334906, ATM-0432565, DGE-0221680 and DOE grant DE-FG02-06ER54887. The Jicamarca Radio Observatory is a facility of the Instituto Geofísico del Perú operated with support from the NSF AGS-0905448 through Cornell University. The authors would like to thank the JRO (and IGP) staff for performing the observations, particularly F. R. Galindo.

[52] Robert Lysak thanks the reviewers for their assistance in evaluating this paper.

References

Campbell-Brown, M. D., and J. Jones (2006), Annual variation of sporadic radar meteor rates, *Mon. Not. R. Astron. Soc.*, *367*(2), 709–716, doi:10.1111/j.1365-2966.2005.09974.x.

Ceplecha, Z., and R. E. McCrosky (1976), Fireball end heights: A diagnostic for the structure of meteoric material, *J. Geophys. Res.*, *81*, 6257–6275, doi:10.1029/JB081i035p06257.

Ceplecha, Z., J. Borovicka, W. G. Elford, D. O. Revelle, R. L. Hawkes, V. Porubcan, and M. Simek (1998), Meteor phenomena and bodies, *Space Sci. Rev.*, *84*, 327–471, doi:10.1023/A:1005069928850.

Chapin, E., and E. Kudeki (1994), Radar interferometric imaging studies of long-duration meteor echoes observed at Jicamarca, *J. Geophys. Res.*, *99* (A5), 8937–8949, doi:10.1029/93JA03198.

Chau, J. L., and R. F. Woodman (2004), Observations of meteor-head echoes using the Jicamarca 50MHz radar in interferometer mode, *Atmos. Chem. Phys. Discuss.*, *4*, 511–521.

Chau, J. L., F. R. Galindo, C. J. Heinselman, and M. J. Nicolls (2009), Meteor-head echo observations using an antenna compression approach with the 450 MHz Poker Flat Incoherent Scatter Radar, *J. Atmos. Sol. Terr. Phys.*, doi:10.1016/j.jastp.2008.08.007.

Close, S., T. Hamlin, M. Oppenheim, L. Cox, and P. Colestock (2008), Dependence of radar signal strength on frequency and aspect angle of nonspecular meteor trails, *J. Geophys. Res.*, *113*, A06203, doi:10.1029/2007JA012647.

Dimant, Y. S., and M. M. Oppenheim (2006a), Meteor trail diffusion and fields in *E* region ionosphere: 1. Simulations, *J. Geophys. Res.*, *111*, A12312, doi:10.1029/2006JA011797.

Dimant, Y. S., and M. M. Oppenheim (2006b), Meteor trail diffusion and fields in *E* region ionosphere: 2. Analytical theory, *J. Geophys. Res.*, *111*, A12313, doi:10.1029/2006JA011798.

Dyrud, L. P., M. M. Oppenheim, S. Close, and S. Hunt (2002), Interpretation of non-specular radar meteor trails, *Geophys. Res. Lett.*, *29*(21), 2012, doi:10.1029/2002GL015953.

Dyrud, L. P., L. Ray, M. Oppenheim, S. Close, and K. Denney (2005), Modeling high-power large-aperture radar meteor trails, *J. Atmos. Sol. Terr. Phys.*, *67*, 1171–1177, doi:10.1016/j.jastp.2005.06.016.

Dyrud, L. P., E. Kudeki, and M. Oppenheim (2007), Modeling long duration meteor trails, *J. Geophys. Res.*, *112*, A12307, doi:10.1029/2007JA012692.

Hedin, A. E. (1991), Extension of the MSIS thermosphere model into the middle and lower atmosphere, *J. Geophys. Res.*, *96*, 1159–1172, doi:10.1029/90JA02125.

Hildebrand, P. H., and R. S. Sekhon (1974), Objective determination of the noise level in Doppler spectra, *J. Appl. Meteorol.*, *13*, 808–811, doi:10.1175/1520-0450(1974)013<0808:ODOTNL>2.0.CO;2.

Kelley, M. C. (2004), A new explanation for long-duration meteor radar echoes: Persistent charged dust trails, *Radio Sci.*, *39*, RS2015, doi:10.1029/2003RS002988.

Larsen, M. F. (2002), Winds and shears in the mesosphere and lower thermosphere: Results from four decades of chemical release wind measurements, *J. Geophys. Res.*, *107*(A8), 1215, doi:10.1029/2001JA000218.

Malhotra, A., and J. D. Mathews (2009), Low-altitude meteor trail echoes, *Geophys. Res. Lett.*, *36*, L21106, doi:10.1029/2009GL040558.

Malhotra, A., J. D. Mathews, and J. V. Urbina (2007), A radio science perspective on long duration meteor trails, *J. Geophys. Res.*, *112*, A12303, doi:10.1029/2007JA012576.

Oppenheim, M. M., L. P. Dyrud, and L. Ray (2003a), Plasma instabilities in meteor trails: Linear theory, *J. Geophys. Res.*, *108*(A2), 1063, doi:10.1029/2002JA009548.

Oppenheim, M. M., L. P. Dyrud, and A. F. vom Endt (2003b), Plasma instabilities in meteor trails: 2-D simulation studies, *J. Geophys. Res.*, *108*(A2), 1064, doi:10.1029/2002JA009549.

Oppenheim, M. M., G. Sugar, E. Bass, Y. S. Dimant, and J. Chau (2008), Day to night variation in meteor trail measurements: Evidence for a new theory of plasma trail evolution, *Geophys. Res. Lett.*, *35*, L03102, doi:10.1029/2007GL032347.

Oppenheim, M. M., G. Sugar, N. O. Slowey, E. Bass, J. L. Chau, and S. Close (2009), Remote sensing lower thermosphere wind profiles using non-specular meteor echoes, *Geophys. Res. Lett.*, *36*, L09817, doi:10.1029/2009GL037353.

Reddi, C. R., T. V. C. Sarma, and P. B. Rao (2002), Spatial domain interferometric VHF radar observations of spread meteor echoes, *J. Atmos. Sol. Terr. Phys.*, *64*, 339–347, doi:10.1016/S1364-6826(01)00107-9.

Zhou, Q.-H., J. D. Mathews, and T. Nakamura (2001), Implications of meteor observations by the MU radar, *Geophys. Res. Lett.*, *28*(7), 1399–1402, doi:10.1029/2000GL012504.

E. Bass, M. M. Oppenheim, and G. Sugar, Center for Space Physics, Boston University, 725 Commonwealth Ave., Boston, MA 02215, USA. (meerso@bu.edu)

J. L. Chau, Radio Observatorio de Jicamarca, Insituto Geofisico del Perú, Apartado 13-0207, Lima 13, Peru.